3D flexure and intraplate compression in the North Sea area

van Wees, J.D.; Cloetingh, S.A.P.L.

published in
Tectonophysics
1996

document version
Publisher's PDF, also known as Version of record

ELSEVIER

Tectonophysics 266 (1996) 343–359

TECTONOPHYSICS

3D Flexure and intraplate compression in the North Sea Basin

J.D. van Wees *, S. Cloetingh

Vrije Universiteit, Instituut van Aardwetenschappen, De Boelelaan 1085, 1081 HV, Amsterdam The Netherlands

Received 30 November 1995; accepted 15 May 1996

Abstract

We apply a recently developed 3D flexure model incorporating lateral variations in flexural rigidity (EET) and necking depth (z_n) to study the 3D effects of intraplate stresses on Quaternary accelerated subsidence and uplift in the North Sea Basin and adjacent areas. In the model approach lateral variations and magnitude of predicted Quaternary vertical motions are largely dependent on the pre-existing Late Tertiary flexural state of the area and the relative change in magnitude and orientation of intraplate stresses in the Quaternary. The Late Tertiary deflections are reconstructed by incorporating lithospheric stretching values calculated from the Mesozoic subsidence record, and by adopting admissible variations in necking depth (z_n) and flexural rigidity (EET) from earlier work. The 3D model results for the North Sea and adjacent areas indicate that an increase of compressive intraplate forces with a magnitude of about 2.25×10^{12} N/m can predict accelerated subsidence values up to 700 m, largely in agreement with observed patterns of Quaternary isopach values corrected for effects of shallowing waterdepth. The magnitude of the intraplate forces is 2 to 3 times lower than predicted by earlier 2D studies. It is believed that the 2D model results actually overestimate required stress levels, since they do not take into account the effect of out-of-plane stresses.The relative increase in compressive forces is in agreement with observed compressive stresses and the magnitude corresponds to characteristic values for plate boundary forces. The adopted values for z_n and EET do not show a clear relation with the preceding basin history.

Keywords: 3D flexure model; intraplate stress; North Sea Basin

1. Introduction

2D studies have shown that lithospheric flexure can be strongly affected by fluctuating intraplate stresses, providing a driving mechanism for short-term large-wavelength modulations in basin subsidence (e.g., Cloetingh et al., 1985). This mechanism is in agreement with observed stress fields, which are relatively constant in orientation over large areas (Zoback et al., 1989), and which can change on relatively short time scales of 1–5 My (Cloetingh and Kooi, 1992). Following the basic assumption that the stress field is uniform, the wavelength and relative amplitudes of stress-induced vertical motions are directly related to the pre-existing flexural state. Thermodynamic models show that flexural loads for rifted basins strongly depend on rheological layering (Braun and Beaumont, 1989; Kooi et al., 1992; Cloetingh et al., 1995). An effective way to translate these effects in forward models for rifted basin formation, is by using a two-step approach, thereby employing the concept of necking depth z_n (Weissel and Karner, 1989; Kooi et al., 1992). First, a kinematically described thinning of the lithosphere

* Corresponding author.

PII S0040-1951(96)00197-7

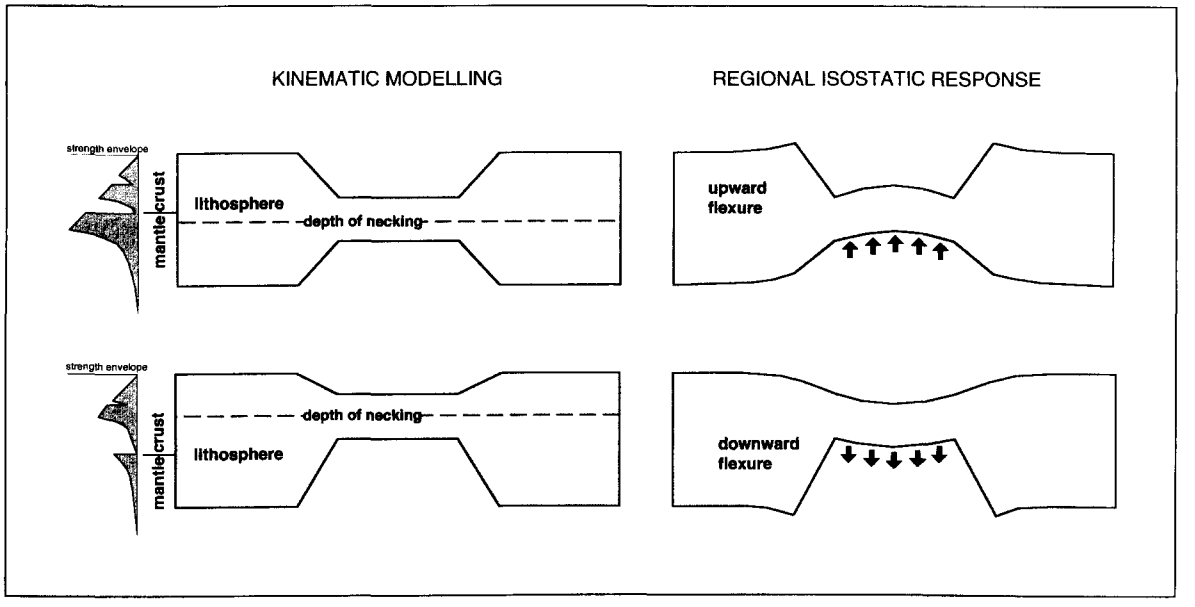

Fig. 1. Concept of lithospheric necking (after Kooi, 1991; modified from Braun and Beaumont, 1989). The level of necking is defined as the level of no vertical motions in the absence of isostatic forces. Left panels, kinematically induced configuration after rifting for different values of necking depth (z_n). Right panels, subsequent flexural rebound.

is applied around z_n in such a way that the depth of necking experiences no vertical deformation in absence of isostatic restoring forces (Fig. 1, left panels). Subsequently, the regional flexural response is a result of buoyancy forces acting on the kinematically perturbed lithosphere, marked by a specific effective elastic thickness (EET) (Fig. 1, right panels). The magnitude of the deflections are determined by lithospheric stretching values and the necking depth z_n, whereas the wavelength of the flexural response is determined by the distribution of effective elastic thickness (EET) (Kooi and Cloetingh, 1992). EET values generally are considered to be function of the rheological composition (Burov and Diament, 1995), but may be strongly affected by stress-induced weakening induced by plastic bending of the lithosphere, which is difficult to assess (Goetze and Evans, 1979; Burov and Diament, 1995). 2D forward basin modelling studies, constrained by basin subsidence, deep seismics and gravity data, indicate that solutions for EET, z_n and lithospheric stretching factors can be non-unique. These models also show that the differences in adopted z_n and EET have a strong influence on the predicted flexural state, whereas associated variations in lithospheric stretching have only a moderate effect on flexure (Kooi and Cloetingh, 1989, 1991, 1992; Karner et al., 1993).

In this paper we apply a recently developed 3D flexure model incorporating lateral variations in flexural rigidity (Van Wees and Cloetingh, 1994; Van Wees et al., 1995) and necking depth to study the 3D effects of intraplate stresses on accelerated subsidence and uplift and compare our results with earlier 2D studies (Kooi et al., 1991). For this purpose we perform a case study on the effect of intraplate stresses on Quaternary subsidence in the North Sea Basin. Quaternary isopach data in the North Sea and adjacent areas, delineated in Fig. 2, provide an excellent database to analyze 3D patterns of accelerated subsidence, deviating from a preceding phase of general tectonic quiescence (Zagwijn, 1989; Kooi et al., 1991).

The Quaternary isopach values show high values up to more than 1000 m aligned along a NNW–SSE axis in the North Sea. Partly, the high values of subsidence may be attributed to non-tectonic effects of shallowing waterdepth and glacial erosion. Comparison of paleo-waterdepth estimates for the Late Tertiary with present-day waterdepth indicates considerable shallowing for the central and south-

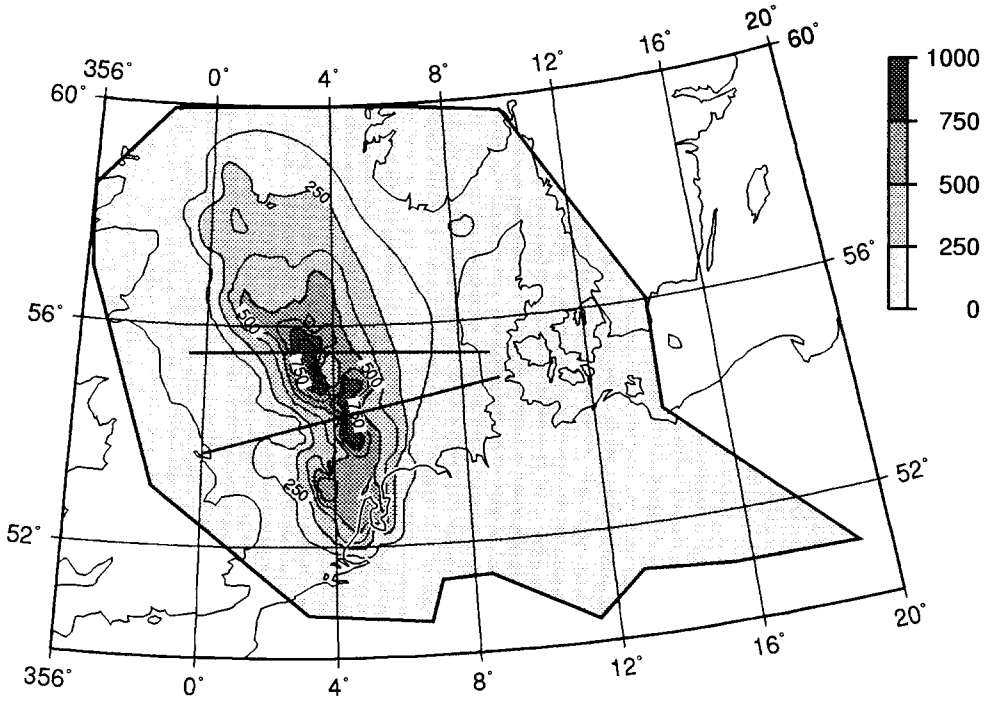

Fig. 2. Quaternary isopach values in the North Sea and adjacent areas. Contour interval is 125 m. In the North Sea and Dutch onshore values have been adopted from compilations of Zagwijn (1989) and Kooi et al. (1991). In the eastern region, Quaternary is assumed negligibly thin (Unesco, 1976; Ziegler, 1990). Solid lines correspond to two cross-sections, for which effects of Quaternary intraplate stress were studied with a 2D model by Kooi et al. (1991).

ern North Sea, reaching maximum values of about 100–150 m (Gradstein et al., 1989; Zagwijn, 1989; Ziegler, 1990). Taking into account large uncertainties in the paleo-waterdepth estimates, suitable variations in adopted shallowing can explain large-wavelength patterns in Quaternary subsidence, up to a maximum of 400 m (Kooi et al., 1991). However, the short-wavelength Quaternary depocentres, marked by a sediment thickness of about 1000 m, require some other mechanism. Alternatively, glacial erosion of pre-Quaternary strata can result in high estimates of tectonic subsidence (Vågnes et al., 1992; Fig. 3). Off the southeast coast of Norway, glaciation probably caused deep post-Mid-Miocene erosion of Tertiary strata (Jensen and Schmidt, 1992), in agreement with a Late Cenozoic bathometric deepening. For the narrow Quaternary depocentres in the central and southern North Sea, which lack indications for deep erosion of Tertiary strata, such a mechanism is unlikely. In the absence of a dominant role of passive mechanisms like changes in water-depth and glacial erosion, the observed accelerated subsidence in these areas must be related to a tectonic process (Cloetingh et al., 1990). Taking into account the well documented present-day compressive stress field in northwestern Europe (Zoback et al., 1989; Zoback, 1992; Müller et al., 1992), revealing a consistently NW–SE orientation of the largest principal stress S_{Hmax} in the delineated region in Fig. 2, Kooi et al. (1991) showed by 2D forward modelling that accelerated subsidence may be attributed to strike-slip (pull apart) deformation or stress-induced downwarping (Fig. 4). More recent 2D studies, focusing on a large number of basins in the northern Atlantic/Mediterranean region marked by Late Cenozoic accelerated tectonic subsidence and simultaneous uplift of basin margins, favour compressional stresses as a driving mechanism for the observed rapid vertical motions (Cloetingh and Kooi, 1992; Reemst et al., 1994). However, it is noted that the 2D models are restricted to narrow areas covered by a limited number of profiles, and

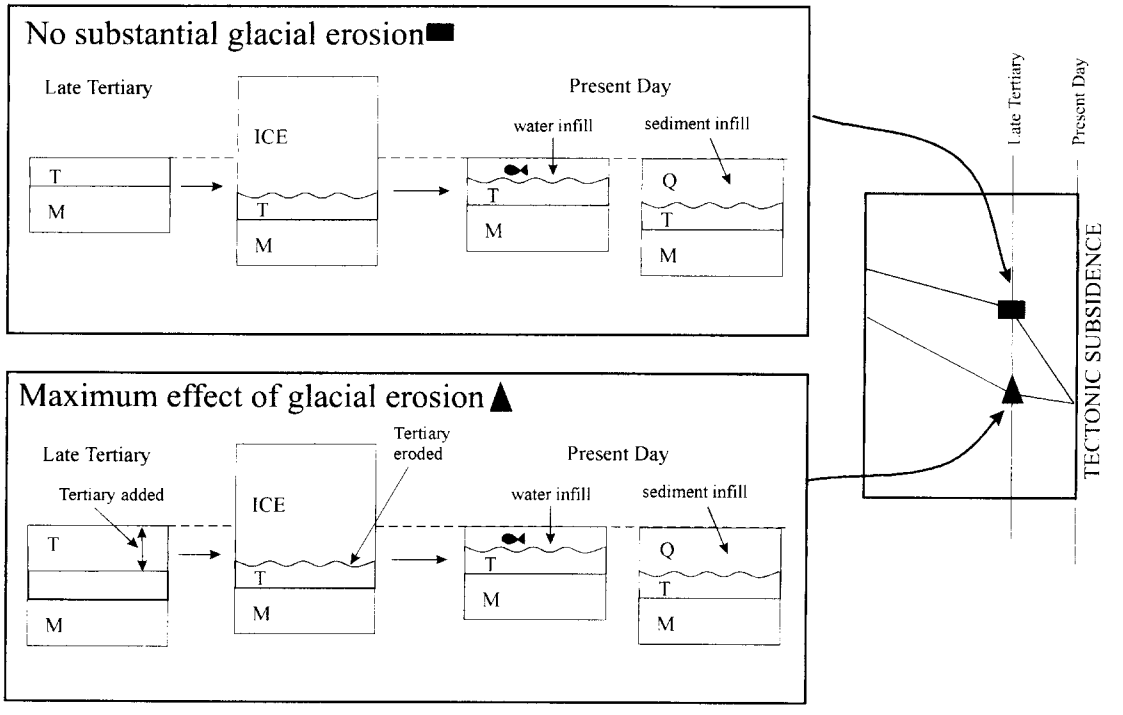

Fig. 3. Potential effect of glacial erosion off the southeast coast of Norway in the calculation of Late Cenozoic tectonic subsidence. In case of no substantial glacial erosion (upper panel), Late Cenozoic increase of waterdepth and/or sediment infill corresponds to a phase of accelerated tectonic subsidence. The amount of air loaded accelerated tectonic subsidence can be locally up to 300–400 m. Considerable glacial erosion (lower panel, note addition and subsequent erosion of Tertiary sediments) results in a depression after glacial rebound, which is filled with water and/or sediments. As a result the reconstructed tectonic subsidence pattern does not show a Late Cenozoic acceleration in subsidence.

neglect out-of-plane stresses, which can substantially contribute to lithospheric flexure. Using the 3D flexure model, it is possible to study basin evolution for a much larger area and to take into account all horizontal components of the stress tensor.

To investigate the effect of intraplate stresses on Quaternary subsidence, it is assumed that the pre-existing flexural state of the area is controlled by the preceding rift history recorded in the Late Permian to Tertiary sediment record, which constitutes the major part of the basin infill (Ziegler, 1990). A first-order approximation of the lithospheric stretching values, in agreement with the observed Late Permian to Tertiary sedimentary record, is obtained by an inverse model for tectonic subsidence values adopting local isostasy (cf. Keen and Dehler, 1993). This allows finding those values admissible for EET and z_n which are best in agreement with stress-induced Quaternary subsidence patterns. Following 2D flexure models (e.g., Kooi et al., 1992), a trial-and-error technique can be used to constrain admissible EET and z_n values and to infer associated modifications of lithospheric stretching parameters compensating flexural loading effects. Here, EET and z_n values are selected from a range of values compiled from earlier flexure studies, in agreement with observed basement warpings, whereas modifications in lithospheric stretching factors derived from local isostasy assumptions are neglected.

2. Late Permian to Tertiary basin evolution and lithospheric stretching values

The well documented Late Permian to Tertiary sediment record in the studied area reflects a complex history of extension and inversion (e.g., Ziegler, 1990). Geological observations and basin analysis show that Late Permian to Early Cretaceous times

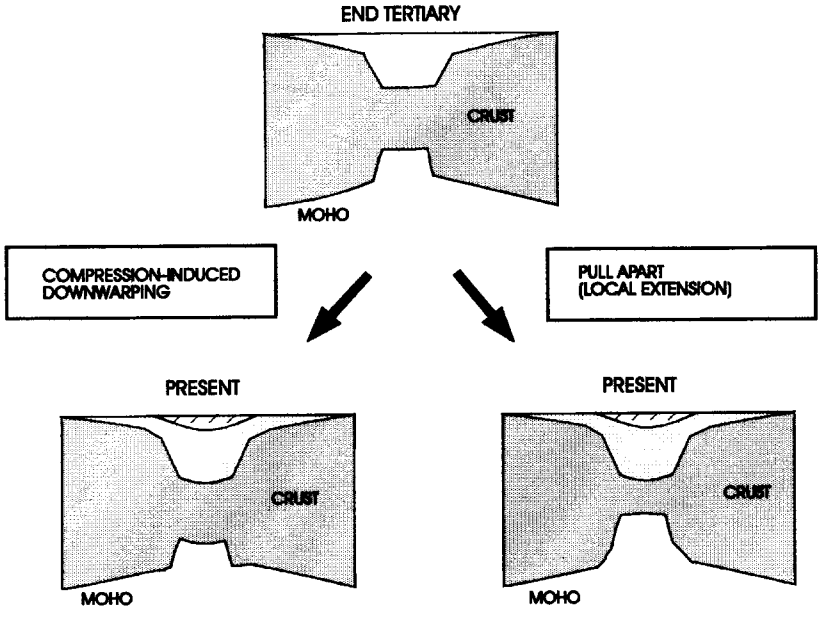

Fig. 4. Schematic illustration of the two mechanisms for the anomalous Quaternary subsidence history in the North Sea (after Kooi et al., 1991). (a) Localised stretching and the development of pull-apart basins. (b) Localised downwarping as a consequence of the modification of the state of flexure of the lithosphere when a change to a more compressional stress level occurs.

are marked by a number of major rift phases (Barton and Wood, 1984; Kooi et al., 1989; Kooi and Cloetingh, 1989; Thorne and Watts, 1989; Ziegler, 1990; Marsden et al., 1990; Hendrie et al., 1993). These resulted in the development of the rift basin elements depicted in Fig. 5, which comprise the Broad Fourteens and West and Central Netherlands Basin (BFWCNB), the Central Graben (CG), the Dutch Central Graben (DCG), the Egersund Basin (EB), the Glückstadt Trough (GT), the Horn Graben (HG), the Lower Saxony Basin (LSB), the Moray Firth Basin (MFB), the Norwegian–Danish Basin (NDB), the Skania Kattegat Basin (SKB) (or Sorgenfrei–Tornquist Zone), the Sole Pit Basin (SPB), and the Viking Graben (VG). The signature and relative importance of the major rift phases, as reflected by tectonic and basement subsidence values, varies strongly for the individual basins (Thorne and Watts, 1989; Ziegler, 1990). Rift activity not only resulted in subsidence. In the Middle and Late Jurassic and Early Cretaceous a number of regional uplift phases occurred, probably induced by rift related thermal doming, which is most evident for the mid North Sea dome at the triple junction of the CG, VG, and MFB (Ziegler, 1990; Hendrie et al., 1993).

Basin analysis indicates that subsidence in the Late Cretaceous and Tertiary, as reflected by the corresponding isopach values (Fig. 6), is primarily driven by a thermal subsidence mechanism (Watts et al., 1982; Kooi and Cloetingh, 1989; Hendrie et al., 1993). However, it is noted that the subsidence patterns may have been affected by intermittent extension and inversion tectonics (Ziegler, 1987; Thorne and Watts, 1989; Zijerveld et al., 1992). Especially in the Lower Saxony Basin and Skania Kattegat Basin the inversion is strong, leading to deep erosion of Mesozoic deposits (Ziegler, 1990).

2.1. Lithospheric stretching

In view of the rift evolution of the area, it is assumed that the Late Tertiary basin configuration is mainly a consequence of rift activity from the Lower Permian to Early Cretaceous. For the Late Tertiary, the thermal effects of rifting will have equilibrated. Consequently, in assessing the rift-induced buoyancy forces for the Late Tertiary state of flexure, it is sufficient to constrain finite crustal stretching factors, since thermally induced buoyancy forces, which may have varied strongly through the rift history as a

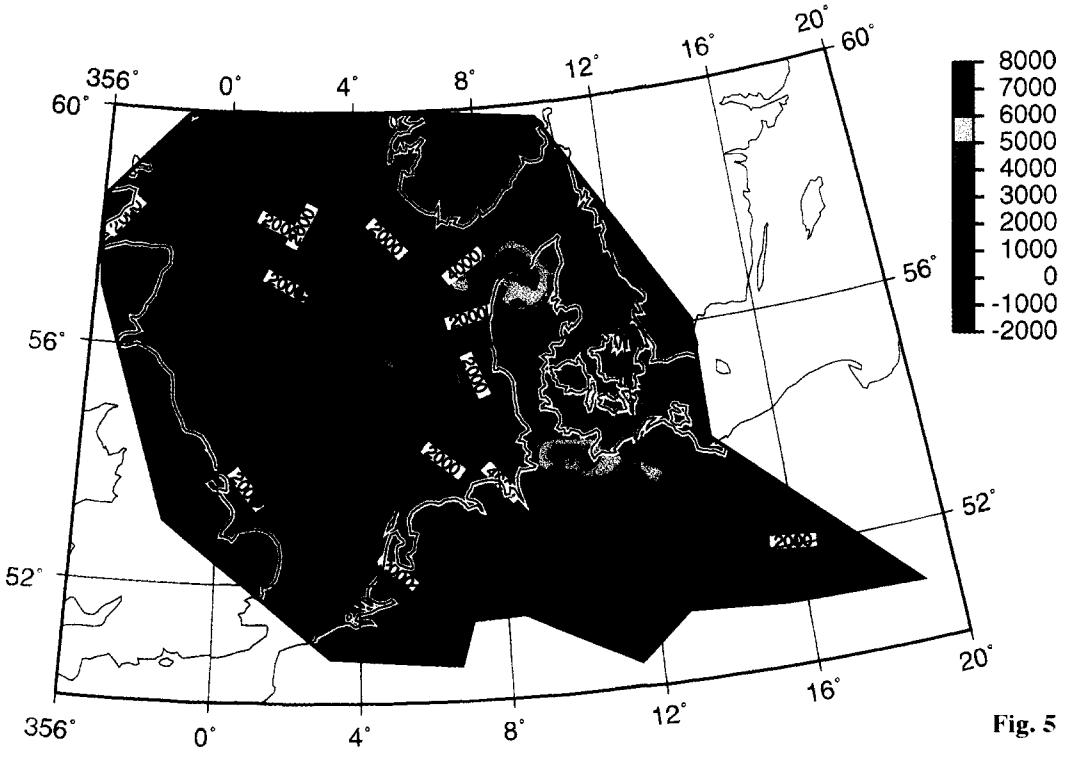
356°
0°
4°
8°
12°
16°
20°
60°
56°
52°
8000
7000
6000
5000
4000
3000
2000
1000
0
-1000
-2000

Fig. 5

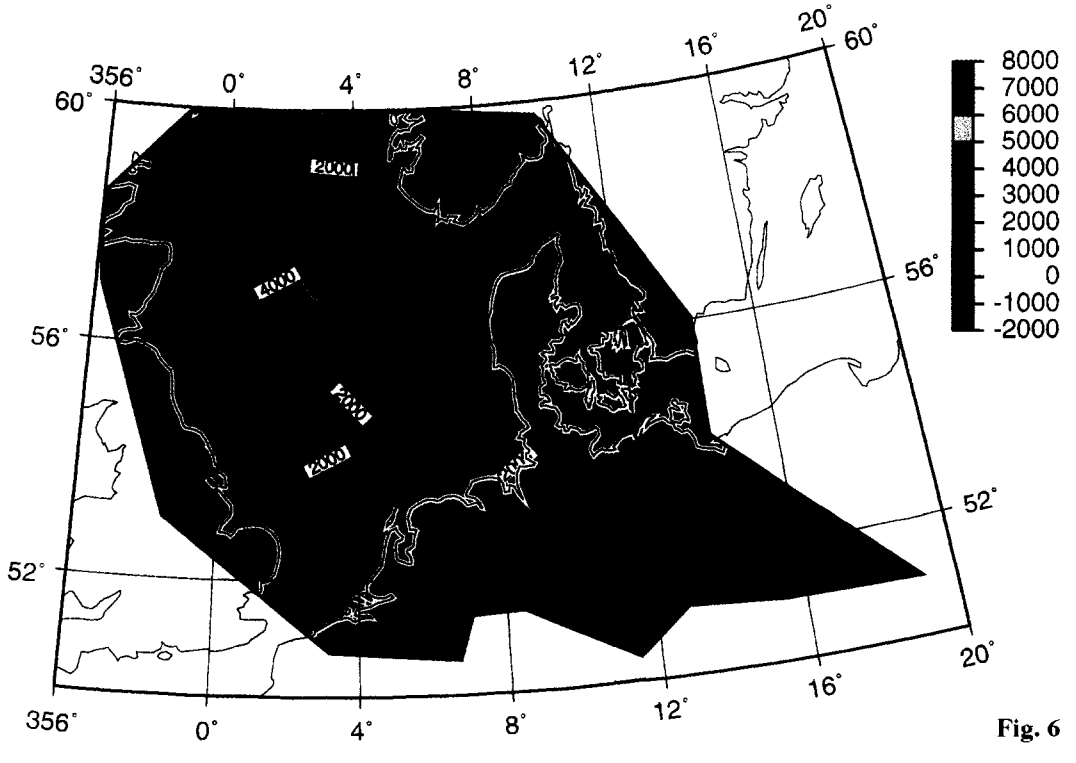
356°
0°
4°
8°
12°
16°
20°
60°
56°
52°
8000
7000
6000
5000
4000
3000
2000
1000
0
-1000
-2000

Fig. 6

Table 1
Model parameters

Symbol	Name	Value
a	initial lithospheric thickness	120 km
c	initial crustal thickness	31 km
T_a	asthenosphere temperature	1333°C
κ	thermal diffusity	7.8×10^{-7} m^2 s^{-1}
ρ_c	surface crustal density	2800 kg m^{-3}
ρ_m	surface mantle density	3300 kg m^{-3}
ρ_w	water density	1030 kg m^{-3}
ρ_s	grain density sediment	2650 kg m^{-3}
ϕ_0	surface porosity	45%
k	depth constant porosity relation	0.4 km^{-1}
α_T	thermal expansion coefficient	3.4×10^{-5}°C
E	Young's modulus	7×0^{10} Nm^2
v	Poisson's ratio	0.25
g	gravity	9.8 m s^{-2}

function of crustal and subcrustal stretching values, will have decayed at this stage.

Adopting local isostasy, assuming thermal equilibration, and neglecting effects of renewed rifting or inversion activity, finite crustal stretching factors for the Late Permian to Early Cretaceous can be calculated directly from the cumulative syn- and postrift tectonic subsidence values derived from the Late Permian to the Tertiary sediment record (e.g., Royden and Keen, 1980; Keen and Dehler, 1993). The cumulative tectonic subsidence in The Late Tertiary is calculated in two steps, adopting parameters listed in Table 1. First, the Late Tertiary isopach values are reconstructed by backstripping the overlying Quaternary sediments. Subsequently the reconstructed sediment thickness values are mapped to tectonic subsidence values, adopting present-day bathometry for Late Tertiary waterdepth. Resulting finite crustal stretching factors are depicted in Fig. 7. They range from 1.00 to 1.58 ($1/\delta$ is 0.63–1.00), and agree very well with the basin framework in the studied area (Fig. 5).

The obtained estimates of crustal stretching can be used to predict present-day crustal thickness values, using the initial crustal thickness of 31 km in Table 1. Adding Late Permian to present sediment thickness values, they form a first-order estimate of Moho depths. Comparison with observed Moho depths in the region (Ziegler, 1990), depicted in Fig. 8, indicates small misfits generally not larger than 4 km, except for the CG, and the southwestern and eastern part of the studied area. High Moho depths for the latter regions, are most likely related to pre-existing thick crust, corresponding to old consolidated crust (Ziegler, 1990). For the CG, Barton and Wood (1984) have suggested that observed extremely shallow Moho depths, compared to predicted values, can be attributed to the pre-existence of thin crust. On the other hand, Kooi et al. (1992) suggested that they can be related to a strong downward flexure of the lithosphere. For other parts misfits may also be attributed to pre-existing variations in crustal thickness or flexural effects.

3. Late Tertiary flexure and stress-induced Quaternary motions

For the 3D flexure calculations a 130×90 grid (spacing $D_x = D_y = 20$ km) is adopted, extending more than 300 km outside the studied region, and the boundary conditions of the model are equal to those used by Van Wees and Cloetingh (1994). Pertinent crustal and subcrustal and sediment parameters are listed in Table 1, and correspond to values adopted in the subsidence analysis. Late Tertiary flexural loading is calculated according to the crustal stretching values derived from local isostasy assumptions in the previous section, assuming effects of thermal uplift to be negligible. For sediment infill in the Late Tertiary, present-day waterdepth is incorporated.

Finite element modelling studies on local stress rotations and the regional stress field, indicate that

Fig. 5. Late Permian to Early Cretaceous 'synrift' isopach values (compiled after data from Ziegler, 1990), reflecting basin framework. Contour interval is 1000 m. Abbreviations correspond to rifted basins: *BFWCNB* = Broad Fourteens and West and Central Netherlands Basin; *CG* = Central Graben; *DCG* = Dutch Central Graben; *EB* = Egersund Basin; *GT* = Glückstadt Trough; *HG* = Horn Graben; *LSB* = Lower Saxony Basin; *MFB* = Moray Firth Basin; *NDB* = Norwegian–Danish Basin; *SKB* = Skania Kattegat Basin (or Sorgenfrei–Tornquist Zone); *SPB* = Sole Pit Basin; *VG* = Viking Graben.

Fig. 6. Late Cretaceous and Tertiary 'postrift' isopach values (compiled after data from Ziegler, 1990). Contour interval is 1000 m. For explanation see text.

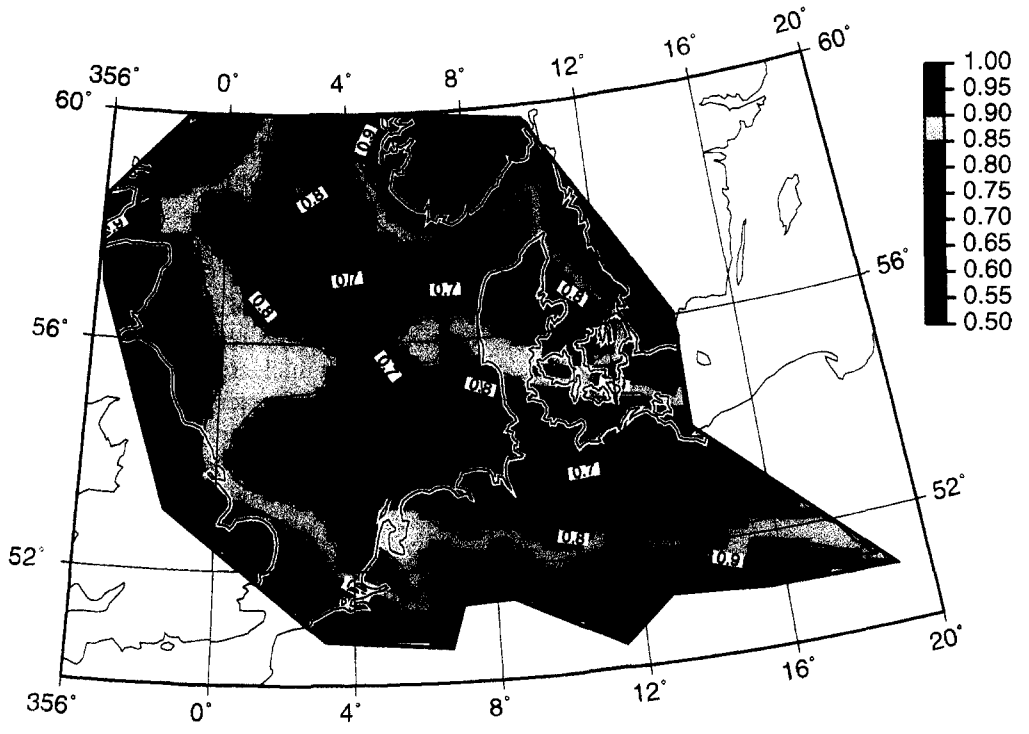

Fig. 7. Finite crustal stretching values ($1/\delta$) in the Late Tertiary, according to accumulative synrift and postrift Late Permian to Tertiary isopach values. Contour interval is 0.05. For explanation see text.

the ratio of principal compressive horizontal stresses S_{Hmax}/S_{hmin} is slightly larger than unity (Grünthal and Stromeyer, 1992; Spann et al., 1994). Here, we adopt compressive forces $T_x = T_y = 2.25 \times 10^{12}$ N/m ($T_{xy} = 0$) for the Quaternary, which is equivalent to a isotropic compressive stress level of 1.5 kbar (150 MPa) in a 15-km-thick elastic plate. The isotropic stresses, which correspond to an absolute minimum value of possible variations in the S_{Hmax}/S_{hmin} ratio, agree best with stress-induced vertical motions along the NNW–SSE axis in the North Sea. The magnitude corresponds to characteristic values for ridge push forces (England and Wortel, 1980) and is in accordance with earlier studies on the effect on intraplate stresses (Kooi and Cloetingh, 1989). In the calculation of the Quaternary stress-induced motions, possible effects of changing waterdepth are not incorporated. As outlined before, shallowing waterdepth may explain large-wavelength patterns in the Quaternary thickness distribution with magnitudes up to 400 m. Consequently, we will primarily aim to predict short-wavelength high-amplitude depocentres in the southern DCG, west of the DCG, and in the western BFWCNB, in agreement with observed isopach values in excess of 400 m and ranging up to 1000 m (Fig. 2).

As outlined in the introduction, the predicted flexural response to the lithospheric stretching values and the effect of Quaternary compressive stresses, is extremely sensitive to the adopted values for EET and z_n. For the North Sea, flexure studies indicate a large range of admissible EET and z_n values in accordance with basin subsidence, deep seismics and gravity data. Constant EET models, incorporating a shallow depth of necking show that observations of basin subsidence in the DCG are consistent with relatively low values for EET of about 10 km (Kooi and Cloetingh, 1989). On the other hand, incorporating a deeper mid crustal level of necking, estimated EET values tend to be much higher, in the order of 20–25 km (Kooi, 1991).

Studies on the CG, incorporating time dependent

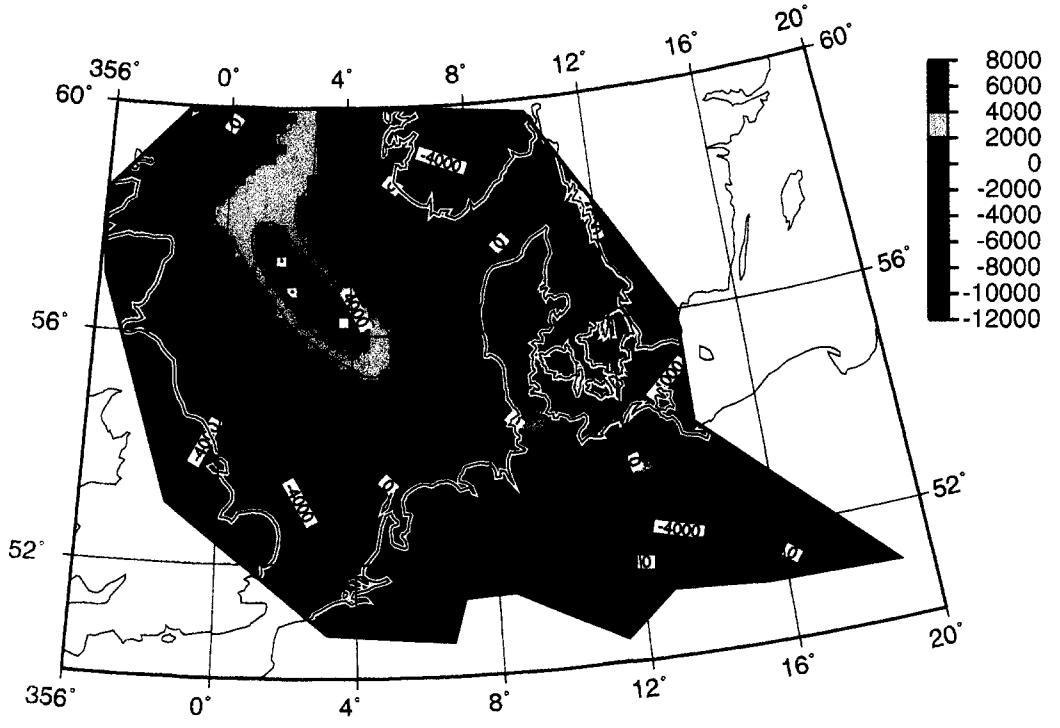

Fig. 8. Difference of Moho depth predicted from crustal stretching values (Fig. 7) and observed Moho depths, adopted from Ziegler (1990). Observed values higher than 35 km, occurring at the southwestern and eastern boundary, have been set to 35 km.

lateral variations in EET, determined by the depth to an isotherm, and incorporating the equivalent of an intermediate necking depth, indicate values for EET of more than 37 km, grading into much lower values of about 23 km in the centre of the basin during the early stages of the rift history (Watts et al., 1982). On the other hand, 3D load-shape analyses for the North Sea, studying present-day lateral variations in EET, incorporating the equivalent of a shallow necking depth, show variations in EET ranging from about 5 to 25 km (Barton and Wood, 1984; Thorne and Watts, 1989). Summarising, the 'z_n models' are subdivided into 2 groups, (1) high constant EET (20–25 km), adopting mid crustal z_n, and (2) low constant EET (10 km) or varying EET (5–30 km), adopting shallow z_n. Conspicuously, both groups reflect only moderate amounts of flexural loading in accordance with low-amplitude gravity anomalies. The CG is probably an exception. Here much higher crustal stretching values than inferred from local isostasy assumptions may have prevailed, in accordance to relatively shallow Moho depths, and significant amounts of downward flexural loading characterised by relatively high EET values (Watts et al., 1982; Thorne and Watts, 1989; Kooi et al., 1992). Present-day heat flow data do not provide arguments in favour of any of the EET models, since they indicate strong deviations of the thermal state of the lithosphere from predictions in rift models, and lack a clear correlation with EET values (Thorne and Watts, 1989). The poor correlation between the thermal state of the lithosphere and predicted EET values may be explained by stress-induced weakening induced by plastic bending of the lithosphere, which is difficult to assess (Goetze and Evans, 1979; Burov and Diament, 1995).

Adopting the previously compiled admissible values, a large range of combinations of EET and z_n values can be incorporated in a 3D flexure model. In the 2D study for the two profiles in Fig. 2, Kooi et al. (1991) adopted an extremely shallow necking depth and lateral variations in EET ranging from 3

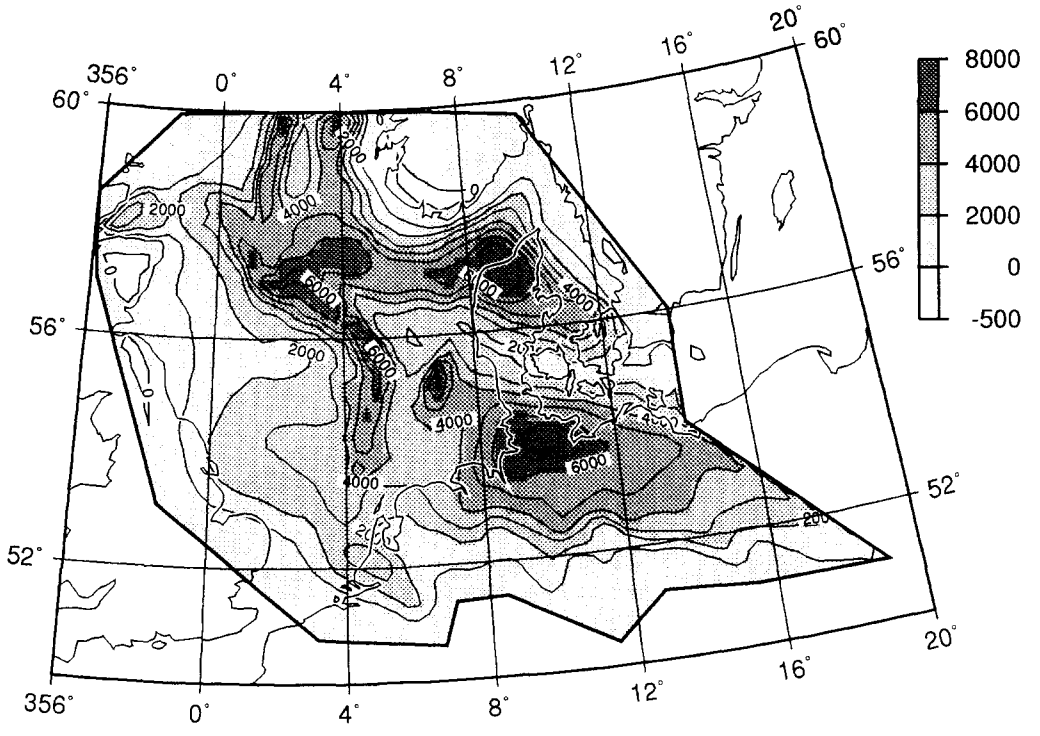

Fig. 9. Late Tertiary reconstruction of basement subsidence (= base Late Permian sediments), obtained from Late Permian to Tertiary isopach values (Figs. 5 and 6), by backstripping overlying Quaternary sediments, and augmented by present-day waterdepth. Contour interval is 1000 m.

km in the Quaternary depocentres to about 20 km at the margins, in agreement with stress-induced Quaternary vertical motions. However, these authors did not compare the predicted values of the preceding Late Tertiary deflections with reconstructed basin subsidence values, rendering the adopted parameters debatable. In fact, the Late Tertiary reconstruction of basin subsidence (Fig. 9), provides much insight in possible variations in EET and z_n. Ragged basement patterns of the basins relative to their margins, strongest developed in the DCG and HG, indicate a relatively deep level of necking or relatively low values for EET (Kooi and Cloetingh, 1989; Kooi, 1991). Outside the depocentres, large-wavelength patterns and uplift of the British Isles and Norway (Doré, 1992), which may have been enhanced by Quaternary compressive stresses, suggest relatively high EET values (Cloetingh and Kooi, 1992). Furthermore, it is noted that local variations of z_n on a scale less than the thickness of the lithosphere are not realistic, since z_n is most likely related to the rheological stratification of the lithosphere (Kooi and Cloetingh, 1992).

In the modelling procedure, by varying EET and z_n in the Late Tertiary flexural reconstruction, we basically try to fit Quaternary subsidence patterns in response to the compressive stress field applied. We check whether adopted EET and z_n results in basement warpings in the Late Tertiary which agree relatively well (first-order fit) with basement reconstruction from backstripping. Since we adopt for the Late Tertiary flexural state crustal stretching values derived from local isostasy assumptions, evidently misfits occur in the Late Tertiary basement reconstruction. We do not attempt to vary crustal stretching values to get a perfect fit for the Late Tertiary, since this is extremely difficult and has a relatively minor effect on the stress-induced motions in the Quaternary, compared to variations in EET and z_n.

At this stage, it is not possible to constrain those values for EET and z_n which agree best with both the Late Tertiary reconstruction and stress-induced Quaternary motions. Therefore, we will start with a constant EET and constant z_n model, corresponding to intermediate values in the range listed above. Based on large misfits in Late Tertiary subsidence and Quaternary stress-induced motions, this model will be improved.

3.1. Constant EET, constant z_n model

For a starting model, the Late Tertiary 3D state of flexure of the North Sea and adjacent areas is reconstructed using a constant EET of 15 km and a constant z_n of 10 km. 3D flexure modelling predictions for the Late Tertiary basement subsidence and Quaternary and the relative motions of the basement in the Quaternary are depicted in Fig. 10. The Late Tertiary model predictions (Fig. 10a) agree fairly well with reconstructed subsidence values, reflecting similar patterns. Large-wavelength deflections, predicting uplift in Norway and parts of the British Isles, are very well in agreement with observations (Doré, 1992; Cloetingh and Kooi, 1992; Riis and Fjeldskaar, 1992). However, model predictions for basement subsidence in the basin depocentres show consistently low subsidence values compared to observed values.

The predicted distribution for accelerated basement subsidence in the Quaternary (Fig. 10b) hardly agrees with short-wavelength and high-amplitude isopach values in the southern DCG, west of the DCG and the western part of the BFWCNB. Instead, maximum values of predicted subsidence correspond to basin depocentres which are marked by large-wavelength Late Tertiary basement subsidence (CG, GT, NDB). Clearly the adopted parameters for lithospheric stretching, EET and z_n are not consistent with reconstructed subsidence patterns in the Late Tertiary and accelerated Quaternary subsidence in the central and southern North Sea.

3.2. Variable EET, variable z_n model

In order to improve both the Late Tertiary and Quaternary subsidence predictions, we adopt the lateral variations in EET and z_n, depicted in Fig. 11. In the BFWCNB and the southern DCG, reduced values of EET are adopted in order to reproduce the ragged basement subsidence more accurately and to assure a Late Tertiary downward state of flexure in accordance with short-wavelength stress-induced downwarping. For the northern DCG, HG, GT, and NDB, z_n is set to a deeper level of 20 km instead of 10 km, resulting in a nearly isostatic response of basement subsidence in the Tertiary, which is consequently hardly affected by compressive stresses. In the CG, misfits for the Late Tertiary may be primarily related to underestimates of crustal stretching values (Kooi et al., 1992). Therefore, we refrain from improving the predicted Late Tertiary subsidence values by varying EET or z_n in the CG. For the northern edge of the studied area, partly corresponding to the northern part of the VG, we also refrain from improving misfits, since they may be largely attributed to edge effects of the model, failing to take into account loading effects of rift structures continuing outside the studied area.

The flexure results for the variable EET and z_n model, depicted in Fig. 12, show a much better fit than the initial model for constant EET and z_n. The predicted Late Tertiary basin subsidence values are in closer agreement with reconstructed values for most sub-basins. For the Quaternary, stress-induced deflections are marked by short-wavelength, high-amplitude basement subsidence values up to 100 m for the western part of the BFWCNB and up to 700 m for the southern part of the DCG, which agree relatively well with the pattern of observed Quaternary isopach values in excess of 400 m (Fig. 2), not related to shallowing waterdepth. However, the model fails to predict a similar depocentre west of the DCG, where the Quaternary is up to 1000 m thick (Fig. 2). In fact, here the model predictions are marked by stress-induced basement uplift. Variations in EET and the magnitude of the intraplate forces do not tend to improve the results. Large-amplitude and short-wavelength variations in z_n may yield better results; however, such variations are considered unrealistic. We also considered more pronounced reduction of EET values in the order of 1–2 km for the southern DCG and western part of the BFWCNB. Such EET values, to be interpreted to be induced by severe plastic bending effects (cf. Goetze and Evans, 1979), may lead to deflections more than 2

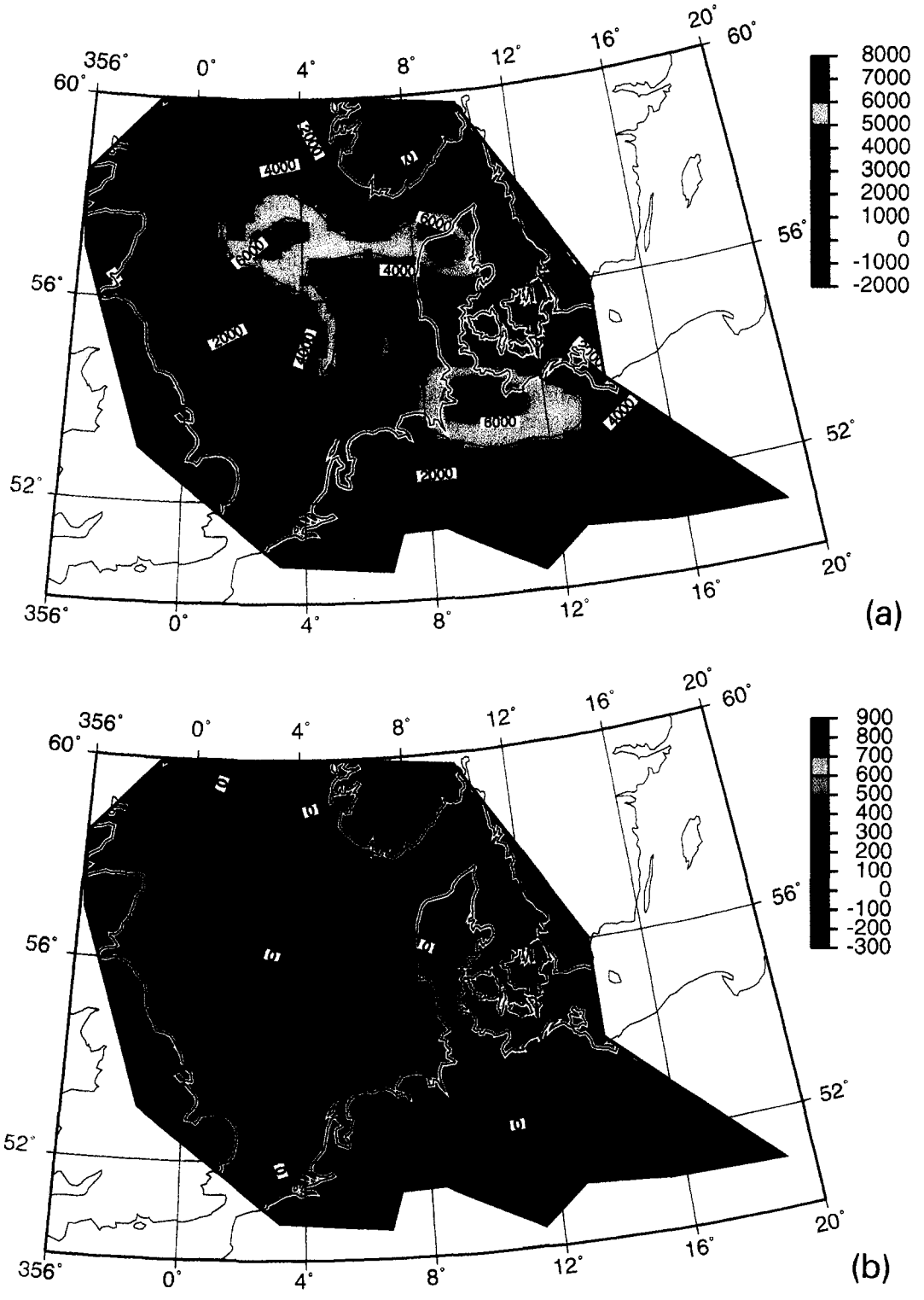

Fig. 10. 3D flexure model results for the Late Tertiary and Quaternary, adopting a constant EET of 15 km and a constant z_0 of 10 km. (a) Predictions of Late Tertiary basement subsidence (= base Late Permian sediments). Contour interval is 1000 m. (b) Stress-induced relative basement motions (contour interval is 50 m).

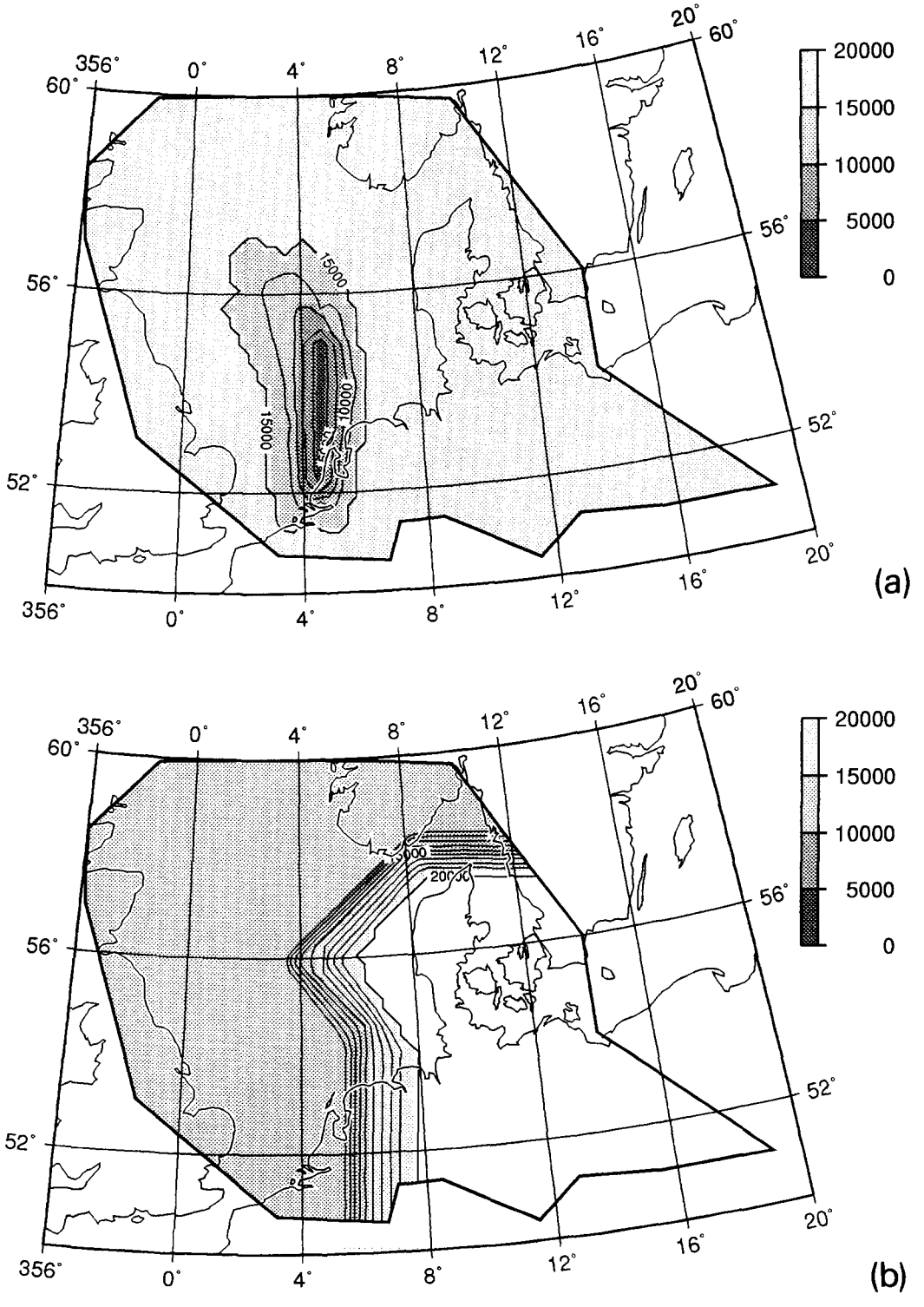

Fig. 11. Improved values for EET and z_n for the 3D flexure model. (a) EET values ranging from 3 km in the southern DCG and BFWCNB to 15 km elsewhere. Contour interval 2500 m. (b) Lateral variations in z_n marked by a region of 20 km (northern DCG, GT, HG, NDB) and 10 km elsewhere. Contour interval 1000 m.

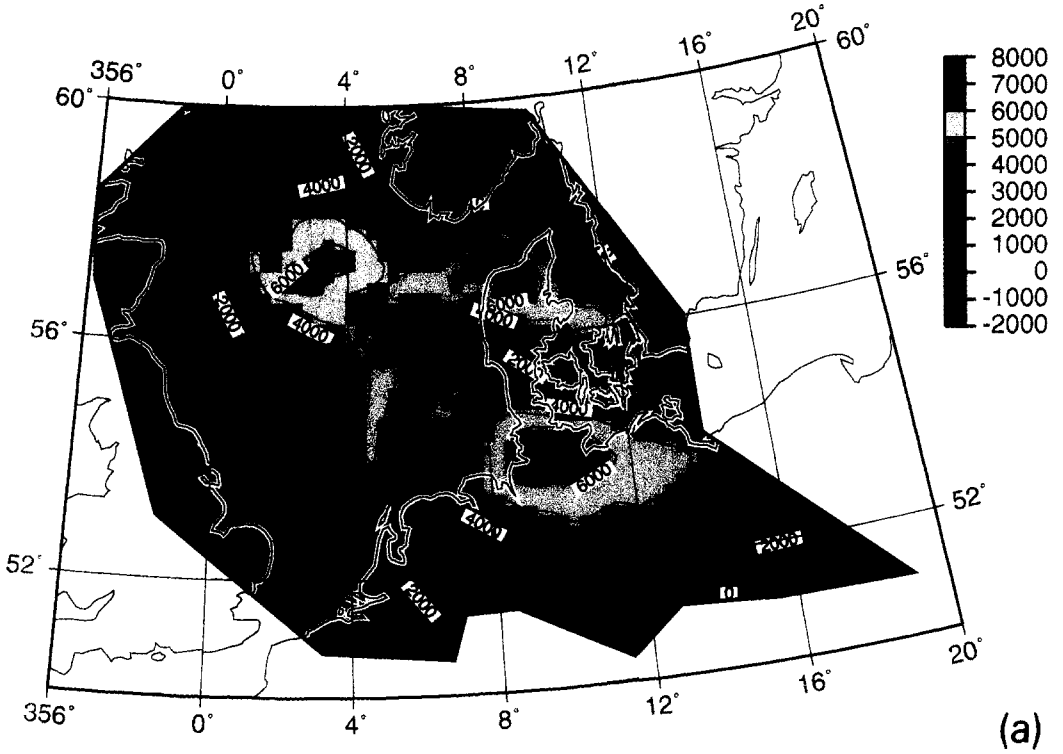
356°
0°
4°
8°
12°
16°
20°
60°
56°
52°
8000
7000
6000
5000
4000
3000
2000
1000
0
-1000
-2000
(a)

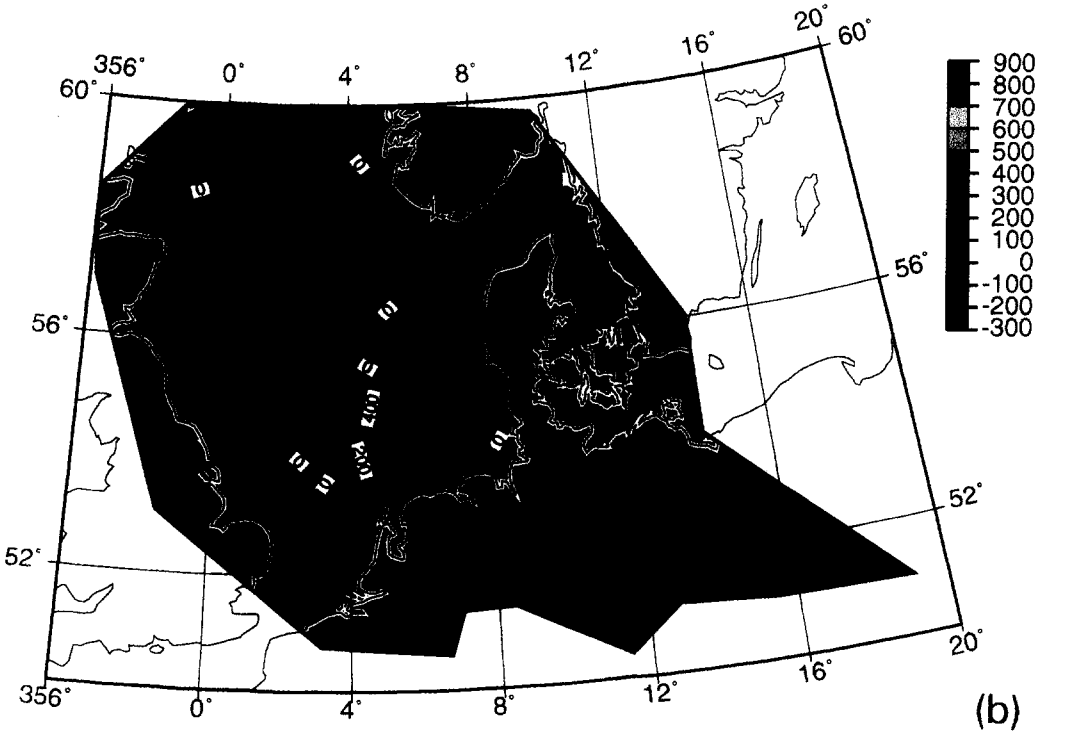
356°
0°
4°
8°
12°
16°
20°
60°
56°
52°
900
800
700
600
500
400
300
200
100
0
-100
-200
-300
(b)

times higher or even infinite, as the intraplate forces approach the bucking limit. However, adopting such low EET values, the width of the zone of downwarping tends to be much smaller than in Fig. 12 and cannot explain the Quaternary subsidence patterns.

The flexure model shows that the intraplate stresses may be a driving mechanism for large basement motions in the order of 700 m, successfully explaining observed Quaternary isopach values in excess of 400 m for large parts of the southern DCG and western part of the BFWCNB. However, the consistent misfit between predicted uplift and observed 1000 m thick isopach values west of the DCG, indicates that here the development of an accentuated Quaternary depocentre cannot be explained by the effect of intraplate stresses. For this domain accelerated Quaternary subsidence is most likely related to an alternative mechanism, like pull-apart extension in a transpressive regime (Kooi et al., 1991; Fig. 4).

4. Conclusions

Adopting admissible variations in z_n and EET, the 3D model results for the North Sea and adjacent areas indicate that a relative increase of compressive intraplate forces with a magnitude of about 2.25×10^{12} N/m can predict accelerated subsidence values up to 700 m, largely in agreement with observed patterns of Quaternary isopach values corrected for effects of shallowing waterdepth. The adopted values for z_n and EET are dictated by the distribution of Quaternary subsidence and consequently they do not show a clear correlation with the rifted basin configuration. With respect to earlier 2D studies on the effect of intraplate stresses, the inferred reduction of EET for the DCG is very similar to variations of EET incorporated by Kooi et al. (1991). With respect to stress levels involved, the latter authors inferred much higher compressive forces of 6×10^{12} N/m, predicting a similar magnitude of subsidence of about 700 m for the Quaternary depocentre in the DCG. It is believed that the 2D model results actually overestimate required stress levels, since they do not take into account the effect of out-of-plane stresses.

Although the model results clearly show that variations of EET and z_n exert a strong control on stress-induced motions, it seems that extreme variations in realistic values for z_n and EET are not capable to explain Quaternary subsidence values over the whole area. Therefore, it is likely that other tectonic mechanisms, like strike-slip deformation (Kooi et al., 1991; Fig. 4), also have played a significant role in Quaternary subsidence.

Fig. 12. 3D flexure model results for the Late Tertiary and Quaternary, adopting lateral variations in EET and z_n depicted in Fig. 11. (a) Predictions of Late Tertiary basement subsidence (= base Late Permian sediments). Contour interval is 1000 m. (b) Stress-induced relative basement motions (contour interval is 100 m).

Acknowledgements

The authors wish to thank Cees Biermann, William Sassi and Randell Stephenson for many useful suggestions and discussions on early drafts of the manuscript. Comments of Caroline Beijdorff and reviews of M. Gölke and E. Burov and two anonymous reviewers are much appreciated. This research was funded by Grant 751.356.023 from the Earth Science Branch (GOA) of the Netherlands Organisation for Research. Publication No. 961101 of the Netherlands Research School of Sedimentary Geology

References

Barton, P. and Wood, R. 1984. Tectonic evolution of the North Sea Basin: crustal stretching and subsidence. Geophys. J. R. Astron. Soc., 79; 987–1022.

Braun, J. and Beaumont, C., 1989. A physical explanation of the relation between flank uplifts and the breakup unconformity at rifted continental margins. Geology, 17: 760–764.

Burov, E.B. and Diament, M., 1995. The effective elastic thickness (T_e) of continental lithosphere: what does it really mean. J. Geophys. Res., 100: 3905–3927.

Cloetingh, S. and Kooi, H., 1992. Intraplate stresses and dynamical aspects of rifted basins. Tectonophysics, 215: 167–185.

Cloetingh, S., McQueen, H. and Lambeck, K., 1985. On a tectonic mechanism for regional sealevel variations. Earth Planet. Sci. Lett., 75: 157–166.

Cloetingh, S., Gradstein, F.M., Kooi, H., Grant, A.C. and Kaminsky, M., 1990. Plate reorganization: a cause of rapid late Neogene subsidence and sedimentation around the North Atlantic? J. Geol. Soc. London, 147: 495–506.

Cloetingh, S., Van Wees, J.D., Van der Beek, P.A. and Spadini, G., 1995. Role of pre-rift rheology in kinematics of extensional basin formation: Constraints from thermomechanical models of mediterranean and intracratonic basins. Mar. Pet. Geol., 12: 793–808.

Doré, A.G., 1992. The Base Tertiary Surface of southern Norway and the northern North Sea. Nor. Geol. Tidsskr., 72: 229–235.

England, P. and Wortel, R., 1980. Some consequences of the subduction of young slabs. Earth Planet. Sci. Lett., 47: 403–415.

Goetze, C. and Evans, B., 1979. Stress and temperature in the bending lithosphere as constrained by experimental rock mechanics. Geophys. J. R. Astron. Soc., 59: 463–478.

Gradstein, F.M., Kaminsky, M.A. and Berggren, W.A., 1989. In: F. Roegl and F.M. Gradstein (Editors), Cenozoic Foraminifera. Vienna, Abh. Geol. Bundesanst., 41: 97–108.

Grünthal, G. and Stromeyer, D., 1992. The recent crustal stress field in central Europe: trajectories and finite element modeling. J. Geophys. Res., 97: 11805–11820.

Hendrie, D.B., Kusznir, N.J. and Hunter, R.H., 1993. Jurassic extension estimates for the North Sea 'triple junction' from flexural backstripping: implications for decompression melting models. Earth Planet. Sci. Lett., 116: 113–127.

Jensen, L.N. and Schmidt, B.J., 1992. Late Tertiary uplift and erosion in the Skagerrak area: magnitude and consequences. Nor. Geol. Tidsskr., 72: 275–280.

Karner, G.D., Driscoll, N.W. and Weissel, J.K., 1993. Response of the lithosphere to in-plane force variations. Earth Planet. Sci. Lett., 114: 397–416.

Keen, C.E. and Dehler, S.A., 1993. Stretching and subsidence: rifting of conjugate margins in the North Atlantic region. Tectonics, 12: 1209–1229.

Kooi, H., 1991. Tectonic modelling of extensional basins: the role of lithospheric flexure, intraplate stress and relative sea-level change. Ph.D. thesis, Vrije Universiteit, Amsterdam, 183 pp.

Kooi, H. and Cloetingh, S., 1989. Intraplate stresses and the tectono-stratigraphic evolution of the Central North Sea. Am. Ass. Pet. Geol. Mem., 46: 541–558.

Kooi, H. and Cloetingh, S., 1992. Lithospheric necking and regional isostasy at extensional basins, 2. Stress-induced vertical motions and relative sea level changes. J. Geophys. Res., 97(B12): 17,573–17,592.

Kooi, H., Cloetingh, S. and Remmelts, G., 1989. Intraplate stresses and the stratigraphic evolution of the North Sea Central Graben. Geol. Mijnbouw, 68: 49–72.

Kooi, H., Hettema, M. and Cloetingh, S., 1991. Lithospheric dynamics and the rapid Pliocene–Quaternary subsidence phase in the southern North Sea Basin. Tectonophysics, 192: 245–259.

Kooi, H., Cloetingh, S. and Burrus, J., 1992. Lithospheric necking and regional isostasy at extensional basins, 1, Subsidence and gravity modelling with an application to the Gulf of Lions Margin (SE France). J. Geophys. Res., 97(B12): 17553–17572.

Marsden, G., Yielding, G., Roberts, A.M. and Kusznir, N.J., 1990. Application of a flexural cantilever simple-shear/pure-shear model of continental extension to the formation of the northern North Sea basin. In: D.J. Blundell and A.D. Gibbs (Editors), Tectonic Evolution of the North Sea Rifts. Oxford Sci. Publ., Oxford, pp. 240–261.

Müller, B., Zoback, M.L., Fuchs, K., Mastin, L., Gregersen, S., Pavoni, N., Stephansson and Ljunggren, C., 1992. Regional patterns of tectonic stress in Europe. J. Geophys. Res., 97: 11783–11804.

Reemst, P., Cloetingh, S. and Fanavoll, S., 1994. Tectono-stratigraphic modelling of Cenozoic uplift and erosion in the SW Barents Sea, Mar. Pet. Geol., 11: 478–490.

Riis, F. and Fjeldskaar, W., 1992. On the magnitude of the Late Tertiary and Quaternary erosion and its significance for the uplift of Scandinavia and the Barents Sea. In: R.M., Larsen, H., Brekke, B.T. Larsen and E. Talleraas (Editors), Structural and Tectonic Modelling and its Application to Petroleum Geology. Nor. Pet. Føren. Spec. Publ. 1. Elsevier, Amsterdam, pp. 163–185.

Royden, L. and Keen, C.E., 1980. Rifting process and thermal evolution of the continental margin of eastern Canada determined from subsidence curves. Earth Planet. Sci. Lett., 51: 343–361.

Spann, H., Müller, B. and Fuchs, K., 1994. Interpretation of anomalies in observed stress data at the Central Graben (North Sea) — numerical and analytical approach. Soil Dyn. Earthquake Eng., 13: 1–11.

Thorne, J.A. and Watts, A.B., 1989. Quantitative analysis of North Sea subsidence. Am. Assoc. Pet. Geol. Bull., 73: 88–116.

Unesco, 1976. Geological World Atlas. Unesco, Paris.

Vågnes, E., Faleide, J.I. and Gudlaugsson, S.T., 1992. Glacial erosion and tectonic uplift in the Barents Sea. Nor. Geol. Tidsskr., 72: 333–338.

Van Wees, J.D. and Cloetingh, S., 1994. A finite difference technique to incorporate spatial variations in rigidity and planar faults into 3-D models for lithospheric flexure. Geophys. J. Int., 117: 179–195.

Van Wees, J.D., Cloetingh, S. and de Vicente, G., 1995. The role of pre-existing weak zones in basin evolution: constraints from 2D finite element and 3D flexure modelling. Geol. Soc. London, Spec. Publ., 99: 297–320.

Watts, A.B., Karner, G.D. and Steckler, M.S., 1982. Lithosphere flexure and the evolution of sedimentary basins. Philos. Trans. R. Soc. London, 305: 249–281.

Weissel, J.K. and Karner, G.D., 1989. Flexural uplift of rift flanks due to mechanical unloading of the lithosphere during extension. J. Geophys. Res., 94: 13919–13950.

Zagwijn, W.H., 1989. The Netherlands during the Tertiary and the Quaternary: a case history of coastal lowland evolution. Geol. Mijnbouw, 68: 107–120.

Ziegler, P., 1987. Late Cretaceous and Cenozoic intra-plate compressional deformations in the Alpine foreland — a geodynamic model. Tectonophysics, 137: 389–420

Ziegler, P., 1990. Geological Atlas of Western and Central Europe. Shell Internationale Petroleum Maatschappij, Den Haag.

Zijerveld, L., Stephenson, R., Cloetingh, S., Duin, E. and Van den Berg, M.W., 1992. Subsidence analysis and modelling of the Roer Valley Graben (SE Netherlands). Tectonophysics,

208: 159–171.
Zoback, M.L., 1992. First- and second-order patterns of stress in the lithosphere: The World Stress Map Project. J. Geophys. Res., 97(B8): 11703–11728.
Zoback, M.L. et al., 1989. Global patterns of tectonic stress. Nature, 341: 291–298.